Pure Appl. Chem., Vol. 82, No. 4, pp. 953–968, 2010.
doi:10.1351/PAC-CON-09-09-17
© 2010 IUPAC, Publication date (Web): 20 March 2010

The larger *N*-heteroacenes*

Uwe H. F. Bunz‡

School of Chemistry and Biochemistry, Georgia Institute of Technology, 901 Atlantic Drive, Atlanta, GA 30332, USA

Abstract: The history and development of pyrazine- and pyridine-type heteroacenes and their use in solid-state organic electronics are discussed and reviewed. The larger *N*-heteroacenes are potential electron- or hole-transporting materials and should therefore complement acenes in organic electronics. As they feature electronegative nitrogen ring atoms in their molecular skeleton, issues with oxidation should be less problematic when comparing them to the larger acenes such as pentacene. This paper covers the synthesis and the solid-state packing of larger (tetracene/pentacene-based) *N*,*N*-heterocylic acenes as well as the question of the interplay of aromaticity and antiaromaticity in the known larger *N*-heteroacenes and their *N*,*N*-dihydro-derivatives; also illuminated are their optical properties. A literature overview is provided.

Keywords: acenes; alkynes; heterocycles; organic chemistry; organic electronics.

INTRODUCTION

Higher acenes have been known since 1929 [1,2] and have emerged as premier materials in organic electronics [3,4]. Anthony's and Wudl's syntheses of soluble and well-characterized higher acene derivatives (hexacene/heptacene) now lead the way to materials with even more promising properties [5–7].

The higher acenes' [8,9] excellent hole-conducting properties and advantageous crystalline packing insure their popularity, and more than 3000 papers dealing with pentacene have appeared according to the *Web of Science* (September 2009), underscoring their practical importance. Pentacene and its derivatives pack in a herringbone pattern that allows for excellent π–π overlap in the solid state. Pentacene's facile and reversible oxidation to its radical cation in the solid state enables its use as a hole-transporting semiconductor. Pentacene's high hole mobility is a result of its good transfer integral (t) and correct nodal overlap of the highest occupied molecular orbitals (HOMOs) of adjacent molecules, as well as a small reorganization energy of the radical cation (λ_+) when going from the neutral molecule to the radical cation [10]. If one allows for heteroatoms (i.e., nitrogen) to be incorporated into the acenes, one should be able to achieve an "Umpolung" of the electric properties of the acenes and heteroacenes may emerge as a class of potentially useful electron-transporting materials. The following account outlines the advances thus far in the study of the larger heteroacenes [11].

Pure Appl. Chem.* **82, 757–1063 (2010). An issue of reviews and research papers based on lectures presented at the 13th International Symposium on Novel Aromatic Compounds (ISNA-13), 19–24 July 2009, Luxembourg City, Luxembourg on the theme of aromaticity.
‡E-mail: ub7@mail.gatech.edu

HISTORICAL OVERVIEW (1870–1990)

Synthesis and structures of larger heteroacenes and their N,N-dihydrogenated congeners [12–16]

Hinsberg synthesized the parent heteroacene systems **3**-H_2, **5**-H_2, **7**-H_2, and **8**-H_2 by melting dihydroxynaphthalene **1** or dichloroquinoxaline **6** with *ortho*-phenylenediamine **2** or 2,3-diamino-naphthalene **4**. Both **3**-H_2 as well as **7**-H_2 were oxidized by acidic chromate into **3** and **7**. Hinsberg noted the strong green–yellow fluorescence of **3**-H_2, **5**-H_2, **7**-H_2, and **8**-H_2 but did not comment upon any fluorescent properties for their oxidation products. The synthesis of **3** and **7** is smooth, but attempts to oxidize **5**-H_2 or **8**-H_2 by chromate failed; undefined materials were obtained. Only in 1967 Kummer and Zimmermann [17] reported azapentacenes via oxidation of **5**-H_2 by chloranil, and of **8**-H_2 by lead dioxide. A copper(I) complex of **7** forms conductive solids but other uses for the fully unsaturated heteroacenes, surprisingly, have not yet emerged [18].

The hydrogenated and "oxidized" *N*-heteroacenes in Schemes 1 and 2 (which show Fischer's homofluorindine and its oxidation by Badger and Pettit [19]) can be classified as $4n$ and $4n + 2$ π-electron perimeters, respectively. The *N*,*N*-dihydro heteroacenes are formally antiaromatic, but the heteroacenes (**3**, **5**, **7**, **8**, etc.) should be aromatic like the linear acenes. This dichotomy apparently escaped attention, and the issue of aromaticity/antiaromaticity in these systems is intriguing. Attempts by Badger [19] to oxidize homofluorindine **10**-H_2 did not yield the aromatic **10** but the quinone **11**. In the late 19th and early 20th centuries, notions of aromaticity or even the aromatic sextet were not yet developed. A distinction in the physical character of the oxidized vs. the reduced species such as the pairs **3/3**-H_2 or **7/7**-H_2 was not investigated. Even later [20], the question of aromaticity in these systems was not contemplated. Homofluorindine, **10**-H_2, displays a structural subtlety. The N–H motif can either be arranged to give an (antiaromatic) dihydropyrazine or as in **10'**-H_2 a quinoid structure. As shown by Dunsch et al. [21] and by Armand et al. [22] using NMR, the "antiaromatic" form, **10**-H_2 is the prevalent one, and the quinoidal form must be there in low or vanishing concentrations. Quantum-chemical calculations (Spartan, B3LYP 6-31G**//B3LYP 6-31G**, without zero point energy (ZPE) correction) corroborate these results, showing that the dihydropyrazine form is 4.2 kcal/mol more stable than the

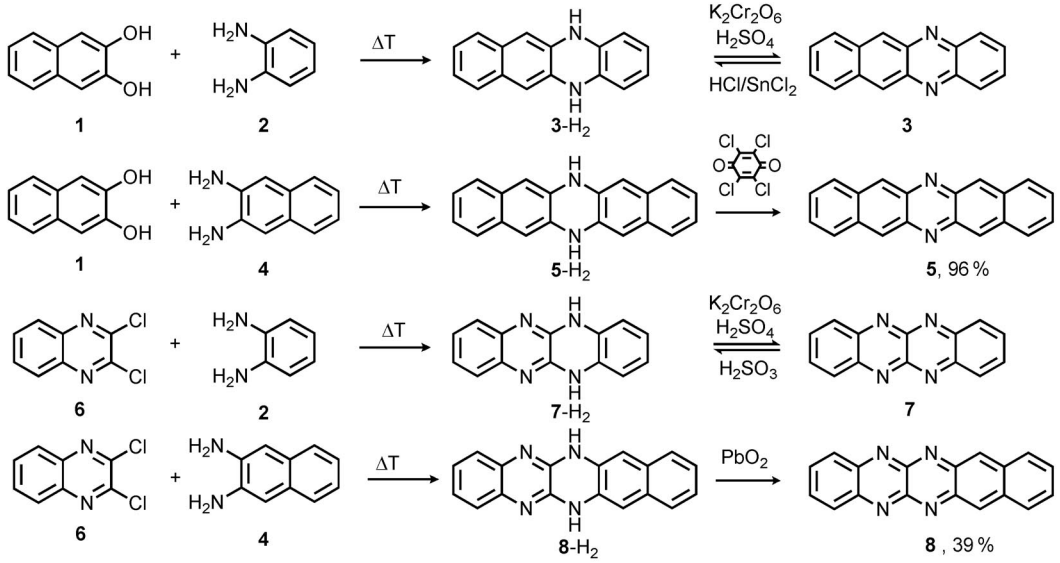

Scheme 1 Synthesis of larger *N*-heteroacenes by Hinsberg and by Kummer and Zimmermann. Yields were not given in Hinsberg's paper.

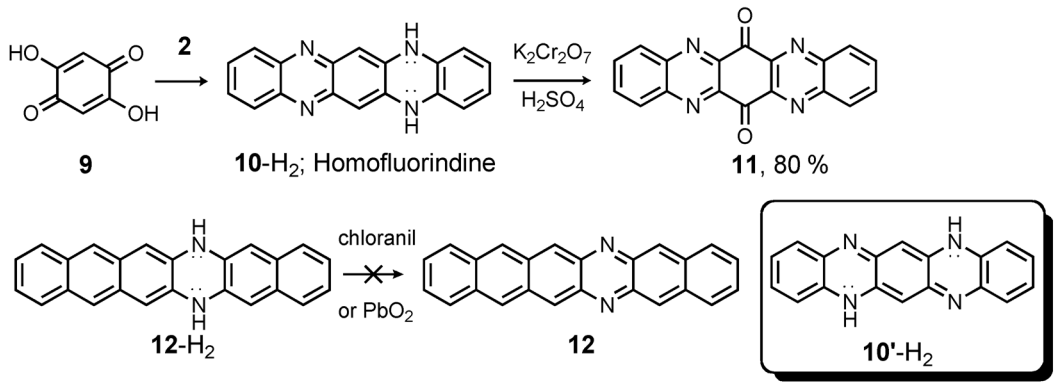

Scheme 2 Attempted syntheses of larger *N*-heteroacenes by Badger et al. and by Kummer and Zimmermann.

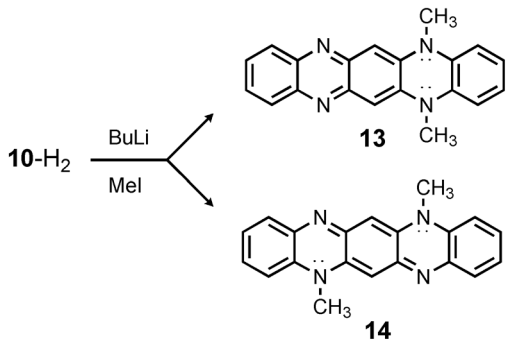

Scheme 3 Synthesis of derivatives of the two tautomers of **10**-H_2 by Miao et al. The compound **13** formed in 55 % yield, while **14** formed in 12 % yield.

quinoidal form **10'**-H_2; **10**-H_2 is somewhat active in organocatalytic hydrogenation reactions as shown by Manassen and Khalif [23]. Tang and Miao [24] quenched the doubly lithiated **10**-H_2 with methyl iodide and obtained a mixture of **13** (55 %) and **14** (12 %), separated by chromatography and characterized by X-ray crystallography (Scheme 3). The predominant formation of **13** is also an indication that **10**-H_2 is more stable than **10'**-H_2. Quinoidal **14** has the smaller bandgap and is planar in the solid state, while **13** is nonplanar as a consequence of the steric demand of the methyl groups when compared to **10**-H_2; the planarity of **14** and the nonplanarity of **13** might also be due to crystal packing effects. A definite answer is currently not available, particularly as Nuckolls showed that the related **5**-H_2 is planar in the solid state. Quantum-chemical methods suggest the larger dihydroheteroacenes are either planar in the gas phase or only slightly pyramidalized, with the planar form only minutely higher in energy [25].

Quast and Schön [26] reported a complementary approach toward larger diazapentacenes, aiming for a different topology than the one incorporating pyrazine units. Pyrazine-derived topologies are always formed by the condensation of an *ortho*-diamine with an *ortho*-quinone or *ortho*-dihydroxyarene. Any two different fragments carrying these functionalities can be joined, but non-pyrazine topologies are not easily available. The base-promoted condensation of **15** with an excess of cyclohexanone furnished **16** in 73 % yield, but **16** was resistant to further attempts of dehydrogenation. Reaction with Pd on charcoal in a sealed tube at 250 °C oxidized **16** to **17** in a mixture with a second product that contained two more hydrogens. Surprisingly, **17** did not undergo further hydrogen loss (Scheme 4).

© 2010, IUPAC

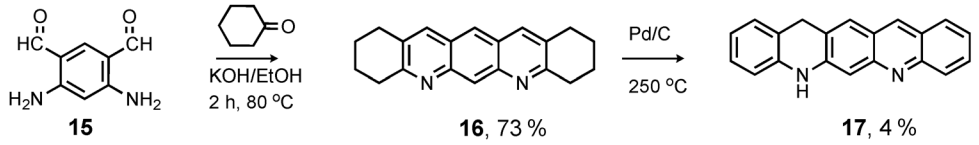

15 **16**, 73 % **17**, 4 %

Scheme 4 Synthesis of dihydrodiazapentacenes by Quast and Schön.

The combination of pyrazines with four-membered rings furnished heterocyclic analogs of the "phenylenes" [27], prepared by Hünig and Pütter [28] (Scheme 5). The intramolecular condensation of **18** leads to the intermediate **19**, which upon deprotonation gives **20** that could not be obtained analytically pure. Amine **20** is a moderately stable green powder, and its oxidation by iodine furnishes **21**, stable and fully characterized with a λ_{max} of absorption at 443 nm. There is a significant blue shift when going from **20** to **21**. From the structure of **20** it is not clear if **20** is aromatic, antiaromatic, or nonaromatic. That is also not clear in the case of **21**, as **20** contains a 22 π-electron system ($4n + 2$), while **21** contains a 20-π perimeter. Both **20** as well as **21** are exciting topologies and warrant further investigation into their structure, aromaticity, and materials properties.

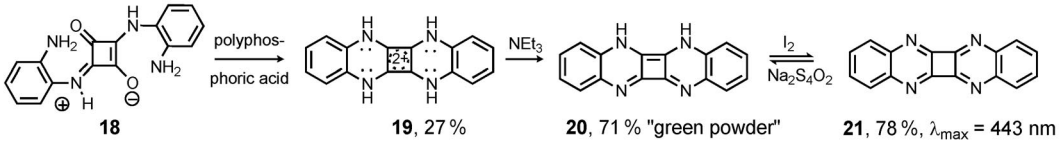

18 **19**, 27 % **20**, 71 % "green powder" **21**, 78 %, λ_{max} = 443 nm

Scheme 5 Synthesis of a cyclobutadiene-containing bisquinoxaline **21** by Hünig and Pütter.

Charging up

Wudl et al. prepared zwitterionic isofluorindines [29], including **22**. Their optical properties were examined, and upon attachment of long alkyl chains (instead of phenyl groups) **22** becomes liquid crystalline. The combination of optical and liquid crystalline properties makes derivatives of **22** potentially interesting in thin film devices. The zwitterionic structure **22** (R = Ph) displays an absorption maximum λ_{max} of 744 nm in ethanol. Upon protonation the absorption is blue-shifted to 660 nm (monoprotonated) and 639 nm (diprotonated) [30]. Inspired by Wudl's work, Siri et al. condensed several aromatic diamines **23** with **9** into **24**, which upon further reaction with a second equivalent of **23** gave substituted fluorindines **25**. In **25**, the lateral positions were appended by halides, methyl groups, or carboxylates (Scheme 6). The absorption maxima of **25** were relatively broad and ranged from a λ_{max} of 550–600 nm, with the longest wavelength absorption for the dihydrotetraazapentacene with four chlorine atoms attached. The electrochemistry was reported, and oxidation occurs between –0.14 and 0.01 V vs. ferrocene/ferrocenium. In the unsymmetrical *N*,*N*-dihydrotetraazapentacenes, prototropic rearrangements, i.e., tautomerization into the alternative dihydropyrazines, are observed during synthesis of the carboxylic acid substituted species [31].

© 2010, IUPAC

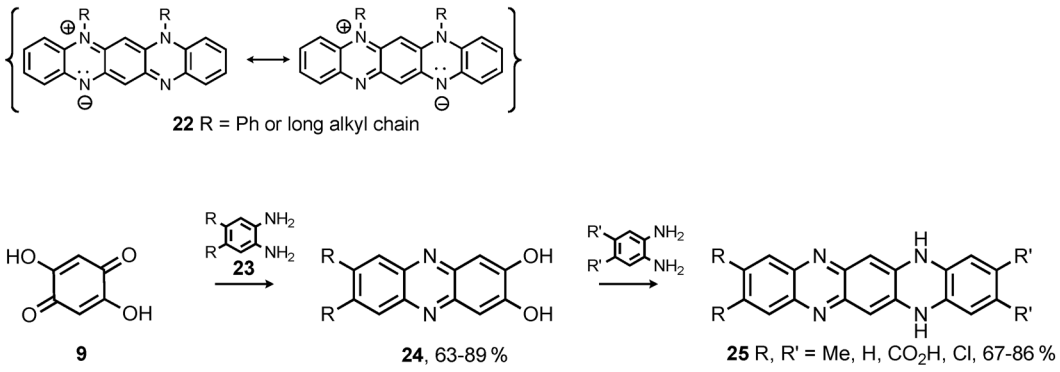

Scheme 6 Synthesis of *N*,*N*-dihydroacenes by Siri et al.

NOVEL DEVELOPMENTS IN HETEROACENES

Nuckolls' heteroacene transistor and Houk's calculations [25,32]

Nuckolls investigated the heteroacene **5**-H_2 and several of its derivatives, including **12**-H_2 for organic electronics applications. He probed their electrical properties and obtained a single-crystal structure of **5**-H_2 and **27**-H_2, which is condensed from **26** and *ortho*-phenylenediamine according to Leete et al. (Scheme 7) [25]. Leete et al. had also succeeded earlier to oxidize **27**-H_2 into **27** (9 % yield) by copper acetate in pyridine [33] as the first reported and characterized example of a diazapentacene, narrowly preceding Zimmermann's report [17].

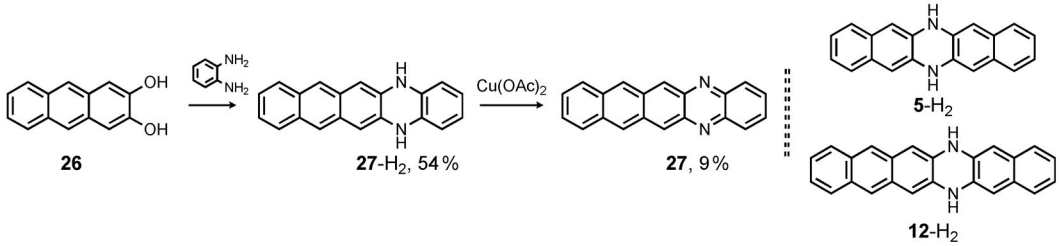

Scheme 7 Synthesis of **27**-H_2 and **27** by Leete et al. and structure of **5**-H_2 and **12**-H_2.

The single-crystal structure of **5**-H_2 (from benzophenone) is similar to that of pentacene, but the molecules are slipped with respect to each other, thereby avoiding the overlap of the dihydropyrazine rings in the solid state. The molecules of **5**-H_2 are planar in the solid state, despite the formally anti-aromatic, central dihydropyrazine ring. In thin films, thermally deposited on SiO_2, **5**-H_2 packs such that its long axis is perpendicular to the solid support, according to powder diffraction data. Thin film transistors of **5**-H_2 and **27**-H_2 were fabricated by thermal evaporation with **27**-H_2 displaying respectable hole mobilities (3–6 × 10^{-3} cm^2 V^{-1} s^{-1}) with excellent on–off ratios. These dihydroheteroacenes do not show sensitivity toward oxidation as observed in pentacene. Their processability is also improved.

The heteroacene **5**-H_2 (re-investigated by Miao et al. [34]) forms three different polymorphs in the solid state and in thin films, of which one has a comparatively high field effect mobility (0.45 cm^2 V^{-1} s^{-1}), making it a contender with pentacene (mobilities up to 35 cm^2 V^{-1} s^{-1}) for most device structures and methodologies [35], particularly as **5**-H_2 is stable and does not undergo oxidative degradation. The high charge-carrier mobility of **5**-H_2 is explained by the correct packing that allows facile charge transport according to the models of Brédas et al. [36]. Miao et al. observed **5** as a byproduct (around

5 %) in the synthesis of **5**-H_2 [34]. To obtain pure **5**-H_2, the starting *ortho*-naphthalenediamine and *ortho*-dihydroxynaphthalene had to be carefully purified, otherwise some of the dehydrogenated **5** forms as byproduct.

Heteroacenes are potentially attractive as electron-transporting materials in thin film transistors. Houk and Winkler used quantum-chemical calculations (DFT-based methods) to examine nitrogen-rich heteroacenes for their potential in organic electronics. The authors compared **28** (pentacene) with **29a–c** and concluded, in order to obtain good electron-transporting properties, that the proposed azapentacenes should carry at least seven, but better still eight or more nitrogen atoms in their perimeter and/or electronegative substituents such as nitriles, which allow for a graphite-like packing such as in **29b**. Critical parameters are the reorganization energy of the radical anion (λ_) in combination with a high electron affinity. Enforcement of a suitable supramolecular arrangement of these materials should maximize the transfer integral t, as the mobility μ should be related to the electron-transfer rate (K_{ET}) between two molecules, a function of the term that contains the transfer integral t and λ_ (eq. 1). If the absolute temperature T is close to zero, K_{ET} would largely depend on the size of t. If λ_ is very small, K_{ET} and therefore μ would also only be dependant upon t, which is defined by the magnitude and phase of the overlap of the lowest unoccupied molecular orbitals (LUMOs) of neighboring, interacting molecules, as discussed by Brédas et al. [37].

$$\mu \sim K_{ET} \sim t^2\, T^{-1/2} \exp[-(\lambda_/T)] \quad (1)$$

The synthesis of **29a–c** has not been reported [32]. A synthetic problem is the lack of solubilizing substituents in **29a–c**. The isolation, purification, and processing of **29a–c** would be quite difficult, even though sublimation and thermal evaporation might work for both purification and processing.

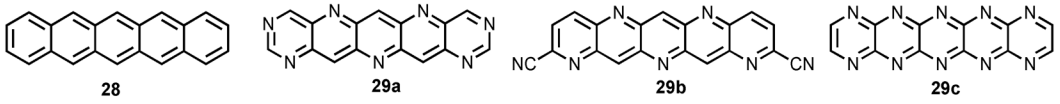

Large pyrazine-containing ribbons and "dog bones"

Wang et al. [38] synthesized large stable pyrazine-containing ribbons (Scheme 8). A clever combination of tetraaminobenzene and pyrenetetrone **30** using alkylated phenylenediamines gave rise to **33** featuring 16 linearly fused six-membered rings. The smaller congeners of **33** such as **34** featuring six or eight benzene rings in a row, are quite fluorescent, but the larger ones are practically nonfluorescent, even though the absorption maximum (chloroform) only shifts from 433 to 538 nm. The fluorescence of the species with 11 rings displays a λ_{max} of 660 nm and a quantum yield of 0.06 [38]. This is surprising, as rigid structures should possess only small Stokes shifts. The absorption spectra of **33** and its smaller congeners display the typical vibronic fine structure expected for rigid molecules, but their emission is broad and featureless. A single-crystal X-ray structure of the smallest target containing six annelated benzene rings was obtained; the intrastack distance is 3.48 Å, which is less than the van der Waals radius, but the molecules are somewhat slipped in the stack with respect to each other [38]. Their first electrochemical reduction potentials range from –1.2 to –0.71 V vs. Ag/AgCl. The largest one, **33**, has a reduction potential of –0.71 V [38], which is close to that of the fullerene derivatives used in photovoltaic cells [39,40]. The stability and the ease of synthesis of **33** and its relatives are due to the interspersed pyrene units. The relatively short absorption wavelength of 538 nm suggests a tetracene-like structure in the ground state with the pyrene units interrupting the conjugation between them. In the excited state, that is apparently not the case anymore, as the emission wavelength is longer. The excited state might be "spread out", perhaps over the whole molecule. Also noticeable is the absence of NH-compounds in this series, which reinforces that, at least in the ground state, these ribbons electronically resemble diaza- or tetraazatetracenes [38].

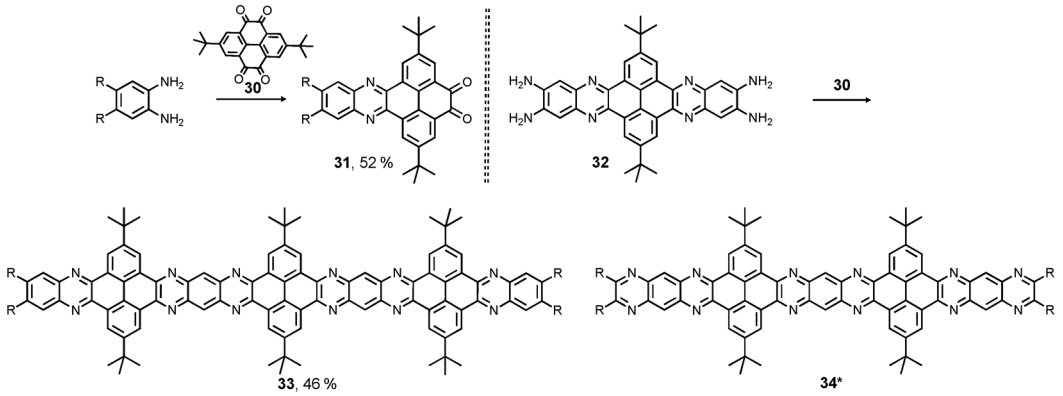

Scheme 8 Synthesis of pyrazine- and pyrene-containing ribbons by Wang et al. (* denotes that smaller oligomers were also produced).

When combined with large planar hydrocarbons, Müllen and Bodwell [41] could embed tetraaza-type pentacenes into large planar, "dog bone"-shaped arenes when starting from the quinone **35a**. These heteroacenes **35b** displays an absorption mximum of 518 nm, while in **35c** the absorption maximum is red-shifted to 660 nm (Scheme 9). Both materials are fluorescent [41]. In the case of phenanthrene-end-capped *N*,*N*-dialkylhexaazapentacenes and *N*,*N*-dialkyloctaazaheptacenes **36b** and **37b**, self-assembly into gel-like and fibrous-crystalline phases has been demonstrated by Hill and Ariga [42].

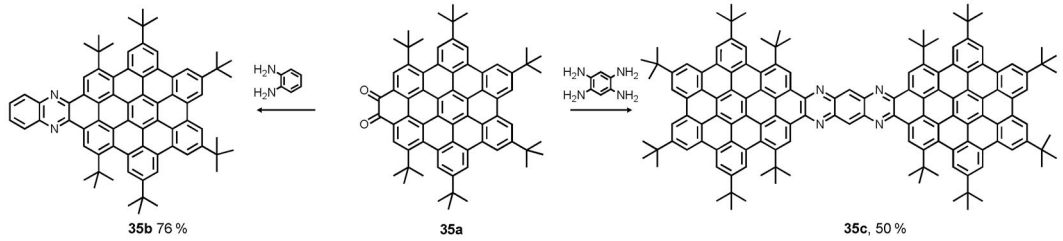

Scheme 9 Synthesis of pyrazine-containing large PAHs by Bodwell and Müllen.

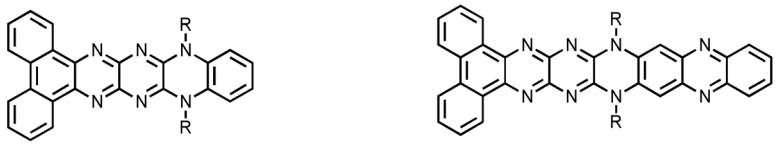

Aromaticity and antiaromaticity in acene-type N-containing heterocycles [43]

The larger heteroacenes and their consanguine *N*,*N*-dihydrocompounds provide a window into the fundamental nature of aromaticity and antiaromaticity, as the number of π-electrons can be increased by two when going from the former to the latter [44]. When looking at Lewis structures and counting π-electrons, the *N*,*N*-dihydroheteroacenes are to be classified as antiaromatic, particularly as they seem to be planar. A useful criterion for the determination of aromaticity is thermochemical, i.e., the heat of hydrogenation of the heteroacenes. The obtained heats of hydrogenation inform about the relative stability of the hydrogenated vs. the fully unsaturated heteroacenes. Independent of that methodology,

magnetic properties can be calculated through the nucleus-independent chemical shift (NICS), which serve as a measure of aromaticity [45]. The hydrogenation of **38** is endothermic, but the hydrogenation of the diazapentacenes **5**, **8**, and **10** is exothermic, even more so than the hydrogenation of pentacene into **41**. Comparing **39** with **5**, it is also apparent that the position of the pyrazine ring plays a role for the heat of hydrogenation (Scheme 10). The dihydroheteroacene **8**-H_2 profits from the formation of the donor–acceptor-stabilized diaminopyrazine motif. Surprisingly, **5**-H_2 and **10**-H_2 also display significant positive, extra cyclic resonance energies (ECREs [46]). The calculated ECREs of the dihydrodiaza- and dihydrotetraazaacenes are larger than those of the respective heteroacenes **5**, **8**, and **10**. This suggests that they are quite stabilized.

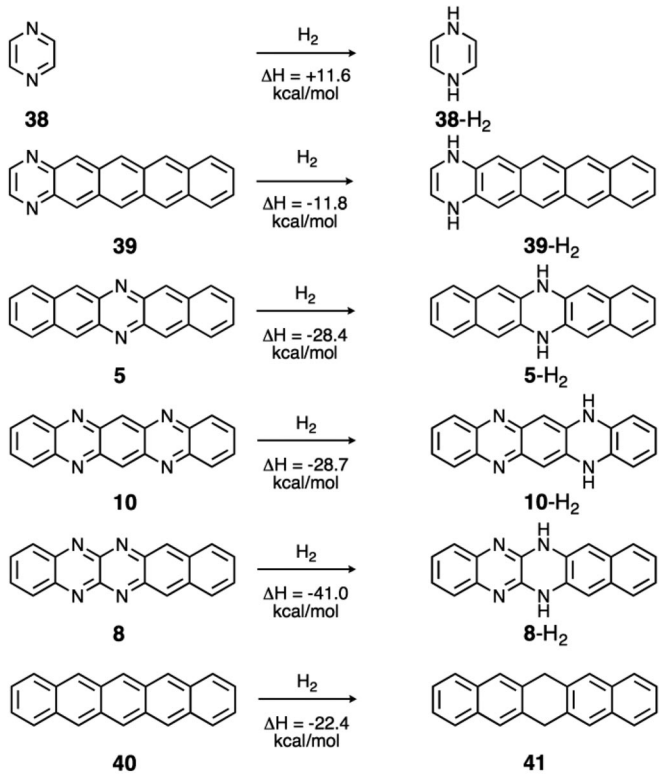

Scheme 10 Heats of hydrogenation for pyrazine **38**, diazapentacenes **5**, **8**, **10**, **39**, and pentacene **40**. All data are computed at the B3LYP/6-311+G** level including ZPE correction. Compounds with a $4n + 2$ π perimeter are traditionally aromatic; formally antiaromatic compounds have a $4n$ π perimeter; according to Bunz, Schleyer et al.

NICS calculations (in collaboration with the group of Schleyer) were performed upon the pairs **10/10**-H_2, and **3/3**-H_2 as representative examples for a tetracene/pentacene and diaza/tetraazaacene (Fig. 1). **3** and **10** display total NICS values that are similar to those obtained for tetracene and pentacene. Heteroatom substitution does not at all perturb aromaticity. Remote contributions to the overall aromatic behavior of **3** and **10** are small but increase the overall aromaticity. "Remote" refers to the influence of the other rings on the aromaticity of the specific ring under consideration. The two dihydroazaacenes **10**-H_2 and **3**-H_2 display an overall reduced aromaticity according to the NICS values; one might argue that **3**-H_2 is even non-aromatic. The 8-π-electron dihydropyrazines are magnetically antiaromatic with NICS values of +23 and +30 for **10**-H_2 and **3**-H_2, respectively. The smaller system unsurprisingly is more antiaromatic than the larger one. The adjacent rings display a slightly reduced local

© 2010, IUPAC

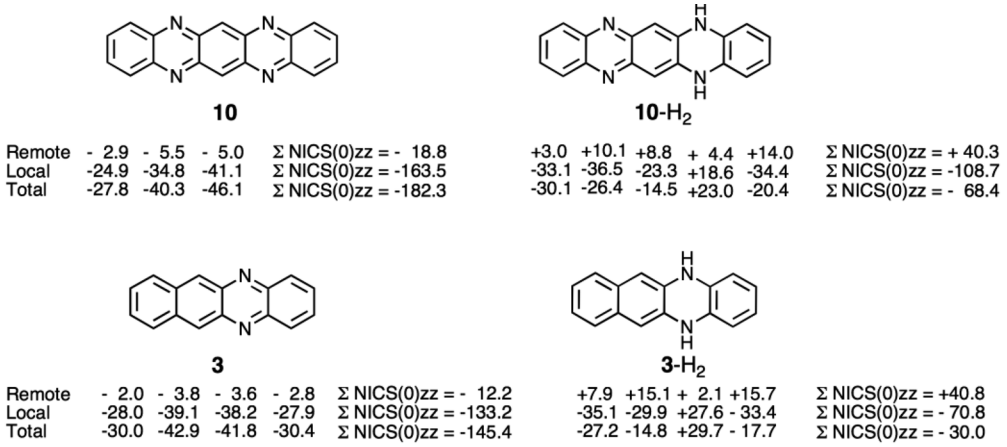

Fig. 1 LMO NICS(0)πzz data (computed at the PW91/IGLOIII//B3LYP/6-311+G** level) according to Bunz, Schleyer et al.

aromaticity and a significantly reduced overall aromaticity. The remote magnetic effects in **10**-H_2 and **3**-H_2 are both of antiaromatic nature, i.e., antiaromaticity is a delocalizing "driving force" and remote effects are larger in the antiaromatic molecules than in the aromatic cases.

Can this be reconciled with the concepts of aromaticity presented in a sophomore organic textbook? One can look at **10**-H_2, for example, as being composed of two independent Clar [1,2] systems, a benzene and an anthracene, similar to the dihydropentacenes (Fig. 2). The two Clar systems are superimposed on an antiaromatic 24-π-electron perimeter. Aromaticity is a localizing force, at least on the scale of a benzene, naphthalene, or anthracene; this is understandable, as smaller aromatic systems are energetically more advantageous. Antiaromaticity is delocalizing, as the larger the perimeter, the 4*n*-π-electrons experience less antiaromatic destabilization. If one looks at simple Hückel calculations, planar cyclooctatetraene is antiaromatic but already slightly stabilized on a "per alkene" basis if compared to ethylene. If the size of the π-system is increased, its aromaticity does not scale with size. This issue is expressed in Clar's rule: a molecule with more explicit benzene rings is more aromatic. An important additional insight would be to view aromaticity not so much as a global property of a molecule, but rather state aromaticity as a property of a specific ring in a multicyclic system.

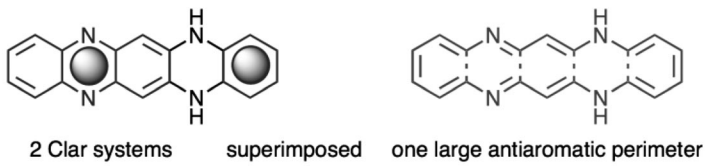

Fig. 2 Aromatic properties of **10**-H_2 might be best explained as a superposition of the localizing effects that the two Clar sextets (gray spheres, left structure) impose and the delocalizing effect that the 20-π-perimeter experiences. This simplified representation is culled from an interpretation of the NICS data of **10**-H_2.

Novel alkynylated diazatetracenes [47] and a dialkynylated tetraazapentacene [48]

Renewed interest in the chemistry of the diazatetracenes and higher azaacenes [49] was heightened by the synthesis of octaethynylphenazine (Scheme 11). A combined condensation/Sonogashira approach starting from tetrabromobenzothiadiazole furnishes **43a** [50,51]. Work in peralkynylated π-perimeters [52] suggested peralkynylated acenes as attractive, but unknown targets. However, peralkynylated

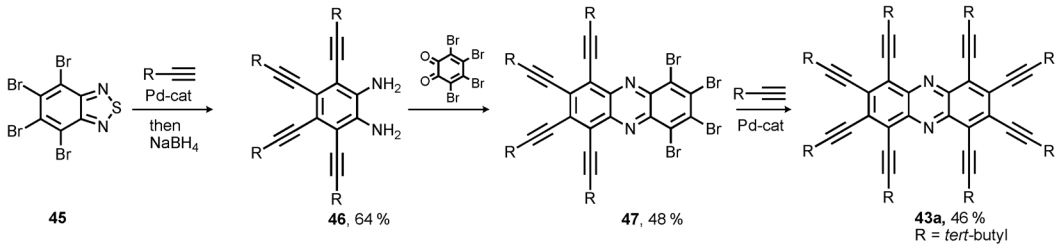

Scheme 11 Synthesis of octaethynylphenazine (R = *t*-butyl) by Miao, Bunz et al.

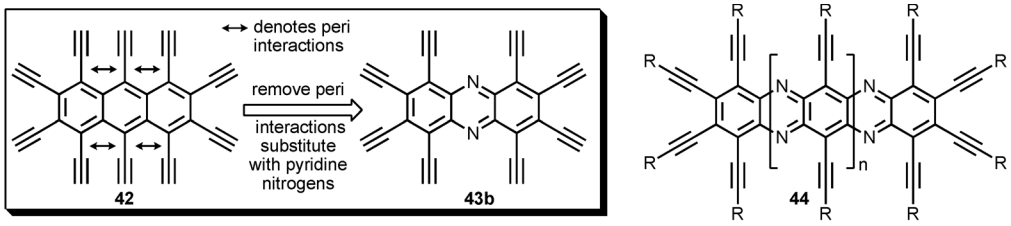

acenes, such as decaethynylanthracene **42** or its substituted derivatives would show severe crowding due to the presence of significant peri-interactions as shown in Fig. 3.

The distortion of the molecular framework caused by the unavoidable peri-interactions between neighboring alkyne substituents (Fig. 3) would make targets such as decaethynylanthracene difficult or impossible to synthesize. To solve this problem, one could introduce pyridine type nitrogens to arrive at structures that are sterically unencumbered, such as the peralkynylated ladder-type materials **44**. As the synthesis of the larger representatives of **44** is challenging due to the lack of suitable starting materials, we envisioned targets with only two alkyne groups placed in the central position of a heteroacene to be more easily accessible. From the standpoint of organic electronics, such targets are attractive, as one expects that their π-faces overlap in the solid state in a similar fashion as Anthony's dialkynylacenes [53].

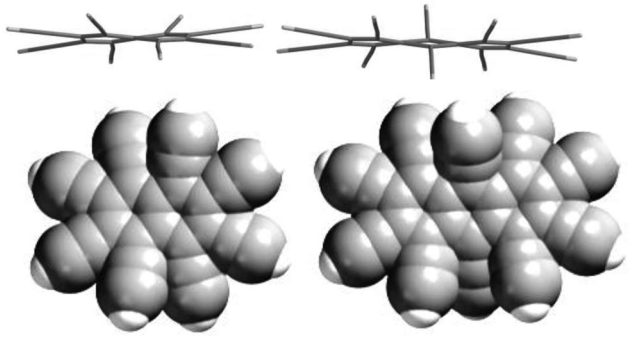

Fig. 3 Molecular design principles for the synthesis of peralkynylated heteroacenes. The inserted double-headed arrows indicate peri interactions (top). Quantum-chemical calculations B3LYP 6-31G**//B3LYP 6-31G** (SPARTAN 08, Windows version) of octaethynylnaphthalene and **42**. These calculations have been performed to obtain correct ground-state geometries. The figures demonstrate the severe distortion of these molecules upon peralkynylation of naphthalene and of anthracene. The middle view shows the molecules as tube models as obtained by SPARTAN, while the bottom view represents the van der Waals (space filling) option for visualization in the same program. Visible are the avoided peri interactions that result by significant twisting of the adjacent alkyne units in the northern and southern parts of the molecules.

© 2010, IUPAC

Scheme 12 shows the synthesis of **50** and **51**. Starting from **48**, a two-step alkynylation furnishes **49a,b**, which upon reduction with lithium aluminum hydride and condensation with *ortho*-quinone gives rise to the isolation of the diazatetracenes **50a,b** in satisfactory overall yields. Reduction of **50a** with hydrogen using Wilkinson's catalyst furnishes **51a**, the *N*,*N*-dihydro-azaacene in near quantitative yield. According to NMR and IR spectroscopy, the reduction is complete, but **51** is quite oxygen-sensitive and, in air, spontaneously reverts back into **50a**, which is stable and can be stored indefinitely.

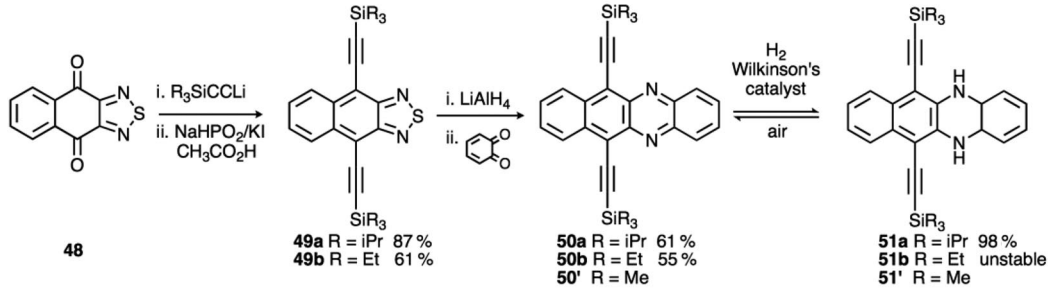

Scheme 12 Synthesis of dialkynylated diazatetracenes by Miao, Bunz et al.

The absorption and the emission spectra of **50a** are red-shifted in comparison to those of **51a** (Fig. 4). While the acene **50a** appears deep orange fluorescent, **51a** is green–yellow fluorescent and shows a distinctly lighter color. The "antiaromatic" system **51a** has a larger bandgap than the aromatic one. Quantum-chemical calculations (B3LYP 6-31G**// B3LYP 6-31G**) were performed on **50'** and **51'** to corroborate the increased bandgap for **51'**, which is due to a significant destabilization of the LUMO upon reduction. The HOMO position, surprisingly, is less influenced. In **50a** and **51a**, the Stokes shifts are small as would be expected for rigid molecular frameworks. The absorption of **50a** displays the typical arene "fingers", vibronic bands that are distinct. A crystal structure of **50b** (Fig. 5) demonstrates that these heteroacenes pack similarly to the analogous acenes prepared by Anthony et al. [5,6].

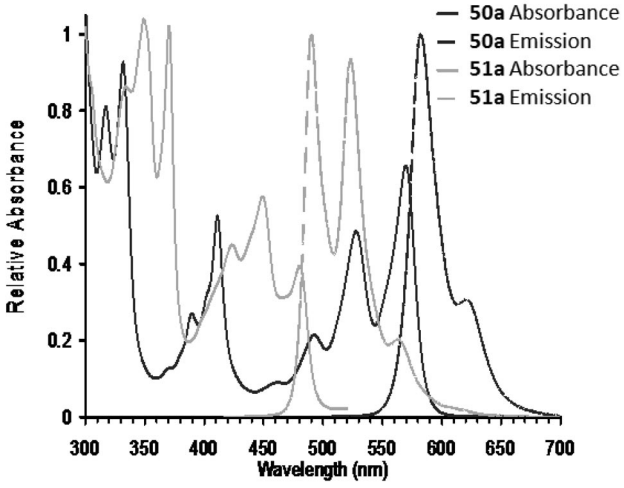

Fig. 4 UV–vis and emission spectra of **50a** and **51a** in dichloromethane according to Miao, Bunz et al.

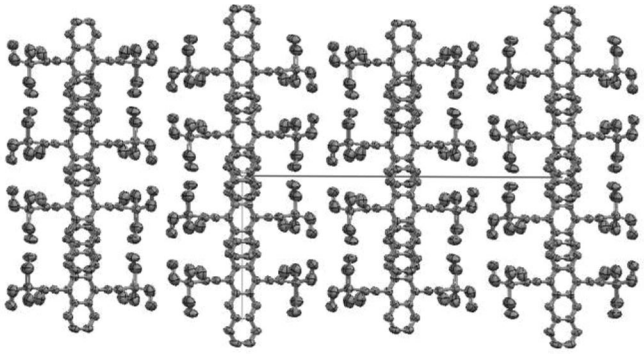

Fig. 5 Packing motif of the diazatetracene derivative **50b** according to Miao, Bunz et al.

Scheme 13 displays the synthesis of the first freely soluble and processible tetraazapentacene **54**. Starting from Badger's quinone **11**, alkynylation with lithio (triisopropylsilyl)ethyne is followed by deoxygenation using the phosphite/iodide reagent combination [54] to obtain the dihydrotetraazapentacene **52**, which is oxidized smoothly with activated manganese dioxide to give **53** as a dark blue, metallic lustrous crystalline material. According to a single-crystal X-ray structure, the molecules of **53** pack in a brick wall motif and stack closely on top of each other. However, the area of overlap between two molecules only includes two rings, but the intrastack distances are small and less than 3.3 Å (Fig. 7). The absorption and emission spectra of **52** and **53** display qualitatively the same trends as observed for **50** and **51** (Figs. 4 and 6), just at lower energies. The absorption and emission of **53** is red-shifted as compared to that of **52** and display a small Stokes shift. In the case of **52**, both absorption and emission are structured with a well-developed fine structure. Particularly, **53** with its red-shifted absorption may be interesting as an active material in photovoltaic applications due to the good overlap with the spectral features of the sunlight.

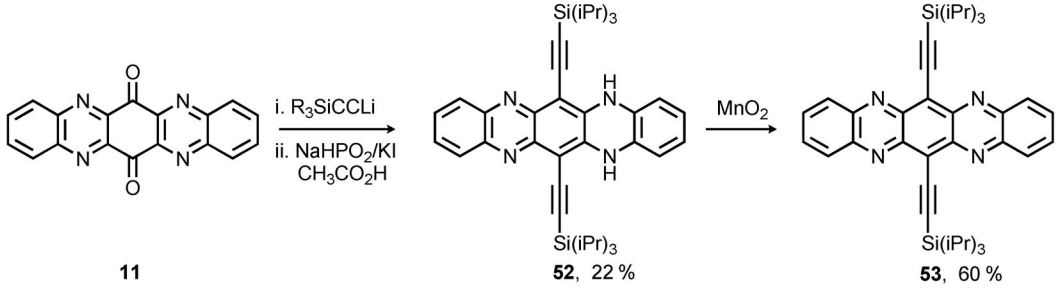

Scheme 13 Synthesis of dialkynylated tetraazapentacenes **52** and **53** by Bunz et al.

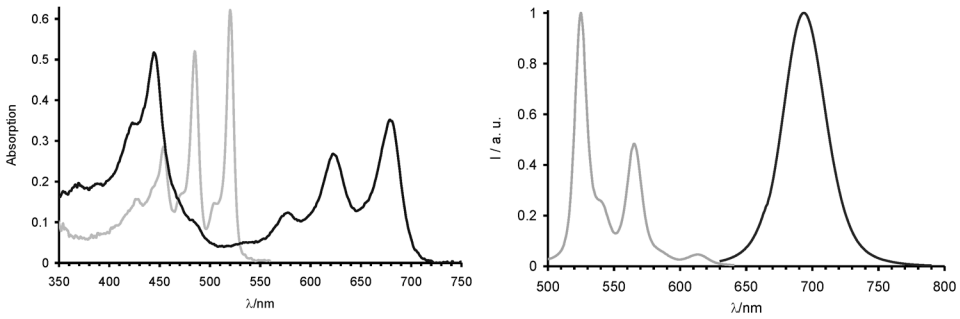

Fig. 6 Absorption (UV–vis) and emission spectra of **52** (gray) and **53** (black) in hexanes according to Miao, Bunz et al.

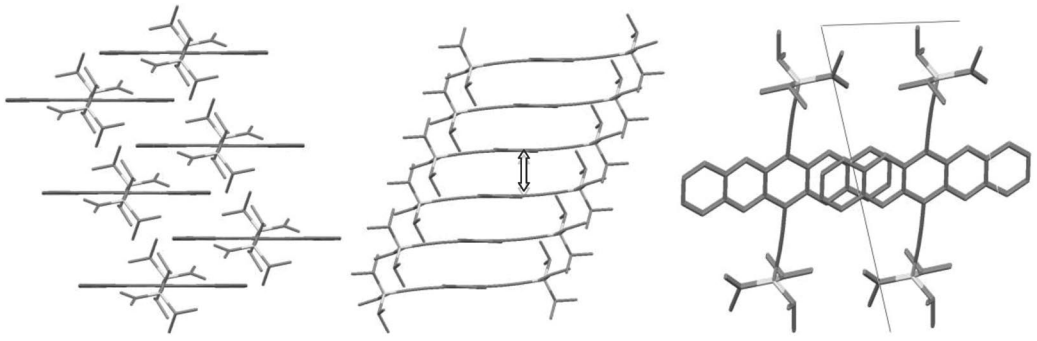

Fig. 7 Packing motif of **53**. While the left and middle representations are not views along a crystallographic axis, the right-hand view shows the stack along the crystallographic *b*-axis, which is not visible, instead the *a*- and *c*-axes are visible as a gray angle. The distance between the molecules in the stacks (middle picture indicated by the up and down arrow) is 3.3 Å according to Miao, Bunz et al.

Cyclic voltammetry of the larger heteroacenes

The larger heteroacenes are pyrazine-type molecules, that is, electron-poor which is reflected in their cyclic voltammetry (Table 1). The hydrogenated species **3**-H_2, **51a** and **52** can be oxidized, but only in the case of **52** reduction (irreversible) is possible at –1.82 V. This is perhaps due to the presence of an intact pyrazine ring. **3**-H_2 features two reversible oxidations, a result of it being the most electron-rich compound. The fully aromatic heteroacenes **3**, **50a**, and **53** cannot be oxidized, but all of them are easily reduced. Having the alkyne groups attached decreases the reduction potential by approximately 0.2 V. Heteroacene **53**, showing four pyridine-type nitrogens as well as two alkyne groups, features a first reduction potential at –0.8 V; this reduction potential is similar to that of fullerene derivatives and might allow the use of **53** in photovoltaic and/or thin film transistor applications if the packing on solid substrates can be controlled. The clear influence of the structure on the electrochemical properties suggests that the reduction potential in larger heteroacenes can be adjusted by the number of nitrogen atoms incorporated into the aromatic skeleton and the overall size of the system. Both increasing size and increasing number of pyridine- or pyrazine-type substituents will lead to lowered reduction potentials when projecting from the current results. Modifications at the perimeter, i.e., introduction of electronegative substituents such as chlorine, nitro or cyano should also significantly increase the electron affinity of the heteroacenes and also modulate their solid-state ordering.

© 2010, IUPAC

Table 1 Electrochemical half-wave potentials (V vs. ferrocenium/ferrocene) for and in THF/0.1 M $^{n}Bu_4N^+PF_6^-$.[a]

Compound	$E_{1/2}(M^{2+/+})$ (V)	$E_{1/2}(M^{+/0})$ (V)	$E_{1/2}(M^{0/-})$ (V)	$E_{1/2}(M^{-/2-})$ (V)
50a	–	–	–1.23[a]	–1.78[a]
3	–	–	–1.44	–2.00[b]
53	–	–	–0.79	–1.23
51a	–	+0.19[b]	–	
3-H$_2$	0.00	–0.21	–	–
52	–	+0.32 [b]	–1.82 [b]	–

[a]In CH_2Cl_2/0.1 M $^{n}Bu_4NPF_6$.
[b]Irreversible.

Potential uses and developments for larger heteroacenes

The most important question for the development of this field is if the heteroacenes will become useful in organic electronic applications. The applications that are most imminent for the heteroacenes would be photovoltaics (the materials are deeply colored and have absorption maxima that range from 500 to almost 700 nm) and thin film transistors; what is necessary to make the heteroacenes fit for organic electronics? To gain some insight, one should compare the heteroacenes to pentacene. One of the major differences would be their use as electron transporters instead of hole transporters. However, it appears to be easier to make a hole transporter due to innate topological differences in their respective orbital phase and its dependency on the number of nodes. The HOMO of a specific material always shows one fewer node than the corresponding LUMO, thereby making *t* potentially larger in hole-conducting materials as the overlap is easier maximized in such a case. The increased number of nodes presents an additional obstacle for the construction of electron transporters that will have to compensated for by possibly making the systems larger and/or controlling the LUMO–LUMO overlap phase through crystal engineering approaches [36,37]. However, if the molecules of the heteroacenes stack in such a way that the LUMO–LUMO interactions are "in phase", this handicap might be minor. One additional way of increasing the magnitude of *t*, the transfer integral, would involve the synthesis of larger heteroacenes, such as tetraaza- or hexaazahexacenes or -heptacenes as such compounds would show larger overlap of the π-faces when carrying bulky substituents. One would assume that the reorganization energies of the heteroacene radical anions are of similar (small) magnitude as those of the radical cations of acenes of identical topology, which is good for charge transport. The demonstrated stability of the heteroacenes to oxidation, is also a real plus for processing and stability. Additionally, the introduction of chloro- or bromo-substituents should be facile, as both tetrachloro*ortho*quinone and tetrabromo*ortho*quinone are commercially available, stable, and should increase the electron affinity of the heteroacenes further.

CONCLUSIONS AND OUTLOOK

Heteroacenes composed of annelated six-membered rings possessing nitrogen ring atoms have a long history, but they have led an existence overshadowed by the "blockbuster" success of pentacene. Overall, the larger heteroacenes are an exciting research topic for the preparative chemist, as the number of reports dealing with substituted (and parent) larger *N*-heteroacenes, other than phenazine and quinoxalines, is small, and the possibility of an electron-transporting version of pentacene quite exciting. This field is currently under-examined as materials with non-pyrazine-type structures are unknown, and *N*-heteroacenes should significantly impact both the organic chemistry of materials as well as organic electronics. An open field is the synthesis of polyazaheteroacenes that do not show the pyrazine-

type topology. For the synthesis of such materials, new synthetic strategies have to be developed or old ones have to be retooled.

ACKNOWLEDGMENTS

I thank the National Science Foundation for generous funding through grant NSF-CHE 0848833 (Heteroacenes, Novel Organic Semiconductors).

REFERENCES

1. E. Clar. *Aromatische Kohlenwasserstoffe*, Springer, Berlin (1941).
2. E. Clar. *Chem. Ber.* **62**, 350 (1929).
3. H. E. Katz, C. Kloc, V. Sundar, J. Zaumseil, A. L. Briseno, Z. Bao. *J. Mater. Res.* **19**, 1995 (2004).
4. C. Reese, Z. A. Bao. *J. Mater. Chem.* **16**, 329 (2006).
5. J. E. Anthony. *Angew. Chem., Int. Ed.* **47**, 452 (2008).
6. J. E. Anthony. *Chem. Rev.* **106**, 5028 (2006).
7. M. M. Payne, S. R. Parkin, J. E. Anthony. *J. Am. Chem. Soc.* **127**, 8028 (2005).
8. D. Chun, Y. Cheng, F. Wudl. *Angew. Chem., Int. Ed.* **47**, 8380 (2008).
9. D. F. Perepichka, M. Bendikov, H. Meng, F. Wudl. *J. Am. Chem. Soc.* **125**, 10190 (2003).
10. J. L. Brédas, J. P. Calbert, D. A. da Silva, J. Cornil. *Proc. Nat. Acad. Sci. USA* **99**, 5804 (2002).
11. U. H. F. Bunz. *Chem.—Eur. J.* **15**, 6780 (2009).
12. O. Hinsberg. *Liebigs Ann. Chem.* **319**, 257 (1901).
13. O. Fischer, E. Hepp. *Chem. Ber.* **23**, 2789 (1890).
14. O. Fischer, E. Hepp. *Chem. Ber.* **28**, 293 (1895).
15. O. N. Witt. *Chem. Ber.* **20**, 1538 (1887).
16. F. Kehrmann, H. Bürgin. *Chem. Ber.* **29**, 1246 (1896).
17. F. Kummer, H. Zimmermann. *Ber. Bunsenges.* **71**, 1119 (1967).
18. M. Tadokoro, S. Yasuzuka, M. Nakamura, T. Shinoda, T. Tatenuma, M. Mitsumi, Y. Ozawa, K. Toriumi, H. Yoshino, D. Shiomi, K. Sato, T. Takui, T. Mori, K. Murata. *Angew. Chem., Int. Ed.* **45**, 5144 (2006).
19. G. M. Badger, R. Pettit. *J. Chem. Soc*. 3211 (1951).
20. S. A. Jenekhe. *Macromolecules* **24**, 1 (1991).
21. L. Sawtschenko, K. Jobst, A. Neudeck L. Dunsch. *Electrochim. Acta* **41**, 123 (1996).
22. J. Armand, L. Boulares, C. Bellec, J. Pinson. *Can. J. Chem.* **65**, 1619 (1987).
23. J. Manassen, Sh. Kalif. *J. Am. Chem. Soc.* **88**, 1943 (1966).
24. Q. Tang, J. Liu, H. S. Chan, Q. Miao. *Chem.—Eur. J.* **15**, 3965 (2009).
25. Q. Miao, T. Q. Nguyen, T. Someya, G. B. Blanchet, C. Nuckolls. *J. Am. Chem. Soc.* **125**, 10284 (2003).
26. H. Quast, N. Schön. *Liebigs Ann. Chem.* 133 (1984).
27. D. Holmes, S. Kumaraswamy, A. J. Matzger, K. P. C. Vollhardt. *Chem.—Eur. J.* **5**, 3399 (1999).
28. S. Hünig, H. Pütter. *Chem. Ber.* **110**, 2532 (1977).
29. F. Wudl, P. A. Koutentis, A. Weitz, B. Mea, T. Strassner, K. N. Houk, S. I. Khan. *Pure Appl. Chem.* **71**, 295 (1999).
30. A. E. Riley, G. W. Mitchell, P. A. Koutentis, M. Bendikov, P. Kaszynski, F. Wudl, S. H. Tolbert. *Adv. Funct. Mater.* **13**, 531 (2003).
31. C. Seillan, H. Brisset, O. Siri. *Org. Lett.* **10**, 4013 (2008).
32. M. Winkler, K. N. Houk. *J. Am. Chem. Soc.* **129**, 1805 (2007).
33. E. Leete, O. Ekechukwu, P. Delvigs. *J. Org. Chem.* **31**, 3734 (1966).
34. Q. Tang, D. Zhang, S. Wang, N. Ke, J. Xu, J. C. Yu, Q. Miao. *Chem. Mater.* **21**, 1400 (2009).
35. O. D. Jurchescu, J. Baas, T. T. M. Palstra. *Appl. Phys. Lett.* **84**, 3061 (2004).

© 2010, IUPAC

36. J.-L. Brédas, D. Beljonne, V. Coropceanu, J. Cornil. *Chem. Rev.* **104**, 4971 (2004).
37. J.-L. Brédas, J. P. Calbert, D. A. da Silva, J. Cornil. *Proc. Nat. Acad. Sci. USA* **99**, 5804 (2002).
38. B. Gao, M. Wang, Y. Cheng, L. Wang, X. Jing, F. Wang. *J. Am. Chem. Soc.* **130**, 8297 (2008).
39. M. Bendikov, F. Wudl, D. F. Perepichka. *Chem. Rev.* **104**, 4891 (2004).
40. D. Dubois, G. Moninot, W. Kutner, M. T. Jones, K. M. Kadish. *J. Phys. Chem.* **96**, 7137 (1992).
41. Y. Fogel, M. Kastler, Z. Wang, D. Andrienko, G. J. Bodwell, K. Müllen. *J. Am. Chem. Soc.* **129**, 11743 (2007).
42. G. J. Richards, J. P. Hill, K. Okamoto, A. Shundo, M. Akada, M. R. J. Elsegood, T. Mori, K. Ariga. *Langmuir* **25**, 8408 (2009).
43. J. I. Wu, C. S. Wannere, Y. Mo, P. v. R. Schleyer, U. H. F. Bunz. *J. Org. Chem.* **74**, 4343 (2009).
44. G. Binsch. *Naturwissenschaften* **60**, 369 (1973).
45. Z. Chen, C. S. Wannere, C. Corminboeuf, R. Puchta, P. v. R. Schleyer. *Chem. Rev.* **105**, 3842 (2005).
46. Y. R. Mo, P. v. R. Schleyer. *Chem.—Eur. J.* **12**, 2009 (2006).
47. S. Miao, S. M. Brombosz, P. v. R. Schleyer, J. I. Wu, S. Barlow, S. R. Marder, K. I. Hardcastle, U. H. F. Bunz. *J. Am. Chem. Soc.* **130**, 7339 (2008).
48. S. Miao, A. L. Appleton, N. Berger, S. Barlow, S. R. Marder, K. I. Hardcastle, U. H. F. Bunz. *Chem.—Eur. J.* **15**, 4990 (2009).
49. A. L. Appleton, S. Miao, S. M. Brombosz, N. J. Berger, S. Barlow, S. R. Marder, B. M. Lawrence, K. I. Hardcastle, U. H. F. Bunz. *Org. Lett.* **11**, 5222 (2009).
50. S. Miao, C. G. Bangcuyo, M. D. Smith, U. H. F. Bunz. *Angew. Chem., Int. Ed.* **45**, 661 (2006).
51. S. Miao, M. D. Smith, U. H. F. Bunz. *Org. Lett.* **8**, 757 (2006).
52. U. H. F. Bunz. *J. Organomet. Chem.* **683**, 269 (2003).
53. J. E. Anthony, D. L. Eaton, S. R. Parkin. *Org. Lett.* **4**, 15 (2002).
54. S. Miao, P. v. R. Schleyer, J. I. Wu, K. I. Hardcastle, U. H. F. Bunz. *Org. Lett.* **9**, 1073 (2007).

© 2010, IUPAC